

## Lipid Bilayer Structure in the Membrane of *Mycoplasma laidlawii*

DONALD M. ENGELMAN†

*Biophysics Department, King's College  
London, England*

(Received 17 July 1970, and in revised form 11 August 1970)

X-ray diffraction patterns from intact, isolated *Mycoplasma laidlawii* membranes at temperatures above and below the thermal phase transition of the membrane lipids reveal important features of the molecular structure of the membrane.

(1) The presence of the close hexagonal fatty acid chain packing giving rise to a sharp 4.15 Å diffraction line indicates that the membrane lipids are in a bilayer below the thermal phase transition. (2) The characteristics predicted for the diffraction from a lipid bilayer can be identified in the low-angle patterns from intact membranes both above and below the thermal phase transition, and the differences between the patterns are as expected from the changes in the wide-angle pattern. (3) The interpretation of the low-angle patterns is confirmed by changing the average fatty acid chain length and observing the expected changes in the pattern produced by changes in the width of the bilayer. (4) The membrane profile diffraction can be largely accounted for by the lipid bilayer, so the majority of the protein is not located in uniform layers on either side of the bilayer regions of the membrane. (5) The area per lipid molecule is 40 to 45 Å<sup>2</sup> in the membrane bilayer below the transition and 60 to 70 Å<sup>2</sup> above it. Since the lipids are very closely packed, protein cannot penetrate the head group layers below the transition to make hydrophobic contact without disrupting the packing. Furthermore, the lipid-protein interaction does not greatly constrain the spacing of the lipid head groups.

### 1. Introduction

Although the idea that the lipid in biological membrane is arranged in a bimolecular leaflet has existed for some time (Gorter & Grendel, 1925; Danielli & Davson, 1935; Robertson, 1959), there has been no direct proof that membranes contain such structures. An evaluation of the experimental support for the idea shows that the evidence is consistent with a bilayer structure but does not demonstrate it directly (Stoeckenius & Engelman, 1969), and other structures have been proposed which are based on alternative interpretations of the data (Korn, 1966; Lucy, 1964; Kavenau, 1966; Benson, 1966; Lenard & Singer, 1966). In the present paper I present strong evidence that a bilayer is the predominant lipid structure in the membrane of *Mycoplasma laidlawii*.

*M. laidlawii* is a micro-organism which is particularly suitable for membrane structural studies. It has only a single membrane which is easily isolated by osmotic lysis (Razin, 1964) and it lacks the specialized wall structures of the bacteria. The fatty acid composition of the membrane lipids can be varied over a wide range by manipulation of the growth conditions and supplementation of the medium with the desired

† Present address: Department of Molecular Biophysics and Biochemistry, Yale University, New Haven, Conn., U.S.A.

fatty acid (McElhaney & Tourtellotte, 1969). Cholesterol content can also be adjusted from zero to about 12% of the lipid (Razin, Tourtellotte, McElhaney & Pollack, 1966). The lipids of the membrane have been shown by differential scanning calorimetry to undergo a thermal phase transition (Steim, Reinert, Tourtellotte, McElhaney & Rader, 1969). X-ray diffraction analysis has shown that the thermal transition consists of a change of the fatty acid chains from a close-packed hexagonal array at low temperature to a more liquid-like state at higher temperature (Engelman, 1970). The variability of the lipid composition and the properties of the thermal phase transition have been most useful in developing an interpretation of the low-angle X-ray diffraction from isolated membranes.

The observations which I describe below are mainly of the diffraction of X-rays by random dispersions and partially oriented arrays of isolated *M. laidlawii* membranes. The theory of diffraction from the dispersions and its application to a number of systems is presented in a separate publication (Wilkins, Blaurock & Engelman, 1971). An outline of the theory is presented below.

## 2. Theory (Wilkins *et al.*, 1971)

For a random dispersion of sheets with uniform transverse electron density profiles the diffraction pattern is a continuous intensity distribution consisting of rings centred on the direction of the incident beam. The intensity will vary with the Bragg angle ( $\theta$ ), in proportion to the square of the Fourier transform ( $F^2$ ) of the electron density profile of the sheet. The diffracted intensity is spread out more as  $\theta$  increases, ( $F^2$ ) being proportional to  $I \sin^2 \theta$  where  $I$  is the intensity for angle  $\theta$ .

If the electron density profile varies along the sheet, additional intensity will appear superimposed on the profile diffraction. In the case of lipid bilayers this does not create difficulties, since the lipid molecules are spaced close to one another and do not exhibit substantial non-profile diffraction at angles corresponding to spacings larger than 6 Å. If large structures such as globular proteins are present, diffraction at larger spacings will occur; such diffraction can only be resolved from the profile diffraction by orienting the sheets parallel to each other or by concentrating the profile diffraction in Bragg orders by stacking the sheets regularly in local regions of the specimen.

In constructing a model of a bimolecular layer of phospholipid molecules it is assumed that the  $\text{CH}_2$  and terminal  $\text{CH}_3$  groups present in the hydrocarbon fatty acid chains fill the space in the centre of the bilayer and the bilayer is symmetrical. Each group is taken as having the same volume as it occupies in the liquid hydrocarbons (Reiss-Husson & Luzzati, 1964). The volumes of the head groups are taken as the sum of the atomic volumes derived for molecules in aqueous solution (Smiles, 1910). The head groups form layers of electron density higher than water; the fatty acid chains form a layer with lower electron density than water. X-rays scattered from the 2 head group layers interfere to give an amplitude  $H = K \cos(2\pi D\theta/\lambda)$ , where  $D$  is the distance between the centres of the 2 layers. The layer of fatty acid chains gives a negative amplitude  $T$ , which decreases rapidly if the layer is uniform and less rapidly if the terminal methyl groups are localized near the centre to give a narrow region of lower electron density. The total amplitude  $F = H + T$  has a  $\cos(2\pi D\theta/\lambda)$  modulation giving a series of bands with maxima at approximately  $\theta = h\lambda/2D$  where  $h = 1, 2, 3$ . The positions of the maxima, then, can be used to find the peak spacing  $D$ . Experimentally,  $|F|$  is measured as  $I^{\frac{1}{2}} \sin \theta$ . To interpret the  $I^{\frac{1}{2}} \sin \theta$  curves,  $F$  has been calculated for a series of model bilayers so that the presence or absence of the features of bilayer diffraction in the membrane diffraction curves can be ascertained. In Fig. 1(a) and (b),  $F$  is shown for 2 model bilayers with and without localization of the terminal  $\text{CH}_3$  groups. The effect of localising the  $\text{CH}_3$  groups is to increase the bands with  $h$  odd relative to those with  $h$  even. Since the observed intensity is related to  $F^2$ , both positive and negative peaks in  $F$  will appear as positive intensities in the diffraction patterns.

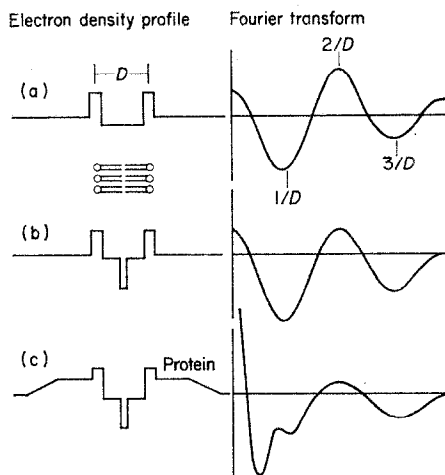


FIG. 1. Fourier transforms of models for bilayer membranes. On the left the electron density is shown vertically *versus* the profile dimension; on the right the amplitude of the corresponding Fourier transform is on the vertical axis *versus* the reciprocal of the equivalent Bragg spacing.

(a) Lipid bilayer with fatty acid terminal methyl groups distributed evenly in the hydrocarbon region.

(b) Lipid bilayer with terminal methyl groups localized at centre of bilayer.

(c) Lipid bilayer with protein layers present on sides of bilayer.

Figure 1(c) shows the effect on the  $F$  curve of adding a thick diffuse region of hydrated protein on either side of the bilayer. The shape of the first band is altered and its maximum shifted to a larger spacing, but the submultiple band positions are unaffected. The finite width of the head group and hydrocarbon layers will also tend to shift the main band position. The submultiple band positions therefore are a better measure of the bilayer thickness than the main band.

The validity of this theoretical treatment has been established by studies of isolated lipids in multilayers (Levine & Wilkins, 1971) and in sonicated aqueous dispersions (Wilkins *et al.*, 1971).

### 3. Materials and Methods

#### (a) *Organism and growth conditions*

*Mycoplasma laidlawii*, strain B (PG9), was grown at 37°C in the lipid-depleted medium of McElhane & Tourtellotte (1969). Supplements of palmitic (hexadecanoic), oleic (*cis*-9-octadecenoic), or erucic (*cis*-13-docosenoic) acids were added to a concentration of 120  $\mu$ M. The static cultures were grown to the late logarithmic growth phase as estimated from turbidity, and harvested by centrifugation at 10,000 g.

#### (b) *Membrane isolation*

Membranes were isolated using the procedure of Razin, Morowitz & Terry (1965). It was found that the osmotic lysis of the organisms was facilitated by osmotic shock at 37°C, probably because of the phase transition in the membrane lipids. The membranes were washed 4 times in a 1:20 dilution of  $\beta$ -buffer ( $\beta$ -buffer is: 0.156 M-NaCl; 0.05 M-Tris; 0.01 M-2-mercaptoethanol, in deionized water, adjusted to pH 7.4 with HCl) by centrifugation and resuspension, brought to 1 mM-NaN<sub>3</sub>, and stored at 4°C.

#### (c) *Fatty acid analysis of lipids*

In order to check the incorporation of fatty acid supplements into the membrane lipids, lipids were extracted from isolated membranes with chloroform-methanol. The extract was evaporated to dryness, resuspended in chloroform, evaporated to dryness, and again resuspended in chloroform. Fatty acid methyl esters were prepared from the extracted

lipids with sodium methoxide (Marinetti, 1962), and analysed on a Perkin-Elmer model F gas-liquid chromatograph. Analyses showed that 65 to 70% of the fatty acids of the membrane lipid consist of the supplemented acid, which is in agreement with the results of McElhaney & Tourtellotte (1969). Average fatty acid chain lengths were obtained for each of the three supplements; they are 16, 17 and 20 carbons for the palmitate, oleate, and erucate supplements, respectively.

#### (d) *X-ray analysis*

Samples were concentrated by centrifugation and sealed into thin glass capillaries of 1 mm diameter. The concentration of material in the specimens was 5 to 10%. The capillaries were then mounted in thermally controlled holders in point-focussing cameras of the Elliott toroid (Elliott, 1965) or Franks (Elliott & Worthington, 1963) type. The Elliott toroid was used for measurement of subsidiary low-angle bands and of the wide-angle pattern; the Franks camera was used to obtain measurements in the low-angle region of 300 to 20 Å equivalent Bragg spacing. Exposures of 2 to 60 hr were taken with  $\text{CuK}\alpha$  radiation. In instances where a series of exposures was required, as in measuring the thermal phase transition characteristics, the initial exposure conditions were repeated at the end of the series. No changes with time or thermal cycling were evident. Films were measured by travelling microscope, vernier calipers, and a Joyce-Loebl microdensitometer.

#### (e) *Electron density profile models*

Step-function models for the membrane electron density profile were developed using the composition of the lipids and the proportion of protein. Electron densities obtained were: methylene chains  $0.320 \text{ e}^-/\text{\AA}^3$ ; terminal methyl groups  $0.180 \text{ e}^-/\text{\AA}^3$ ; lipid head groups  $0.450 \text{ e}^-/\text{\AA}^3$ ; hydrated protein  $0.405 \text{ e}^-/\text{\AA}^3$ . The dimensions of the bilayers shown in Fig. 1 were obtained from measuring Corey-Pauling-Koltun (Koltun, 1965) models of the lipids of a palmitate-enriched membrane. The lipid chains were assumed to be perpendicular to the plane of the bilayer and in the all-*trans* conformation. The values obtained were 38 Å for the hydrocarbon region and 10 Å for the width of a lipid head group region, so the centre-to-centre spacing of the head group regions is 48 Å. Similarly, models were built for the erucate-enriched membrane lipids (average chain length = 20 carbons), and a peak-to-peak spacing of about 55 Å was obtained; however, accommodation of the *cis* double-bond was managed only with some difficulty and the value is less precise than for the palmitate case.

#### (f) *Electron microscopy*

Membranes were prepared for examination in the electron microscope by negative staining with uranyl acetate at temperatures above and below the thermal phase transition. The specimens were examined in a Philips EM300 microscope.

## 4. Results

### (a) *Membrane lipid phase transition*

The existence of a thermal phase transition in the membrane lipids has been demonstrated by differential scanning calorimetry (Steim *et al.*, 1969) and the molecular nature of the transition has been ascertained by X-ray diffraction (Engelman, 1970). The diffraction analysis has been extended and, although the basic interpretation is unchanged, will be reviewed here since it is of great importance in interpreting the low-angle scattering from membrane dispersions.

Organisms were grown in supplemented media to obtain membranes in which the lipids contained palmitic, oleic or erucic acids as the predominant esterified fatty acids. In each of the three membrane types transitions were observed in the X-ray patterns taken at different temperatures. The most prominent feature of the change is a gradual shift from a broad, strong ring centred at 4.6 Å to a sharp, strong ring near

4.15 Å as the temperature is lowered. This change occurs in diffraction from dispersions of isolated lipids and suspensions of intact organisms as well as from isolated membranes. The transition occurs over a broad temperature range. Microdensitometer traces show a gradual disappearance of the broad 4.6 Å peak accompanied by a gradual appearance of the 4.15 Å peak as the temperature is lowered. Since the broad 4.6 Å ring is observed as a shoulder on the side of the strong water diffraction ring at 3.3 Å, it is difficult to detect the low temperature end of the transition at which the 4.6 Å ring disappears, and improved measurements show that the transition is substantially broader than the 8 to 10°C previously reported (Engelman, 1970). The high temperature end of the transition, in contrast, can be measured with considerable accuracy since it is marked by the disappearance of a sharp ring against a diffuse background.

In spite of the measurement difficulty, it is apparent that at least 80% of the lipid chain diffraction in the wide-angle region is involved with the transition. This is in agreement with the results of Reinert & Steim (1970), whose differential scanning calorimetric measurements show that essentially all of the lipid chains present are involved in the transition.

In each of the three types of membrane the transition occurs over a different temperature range. The high temperature ends of the transitions are at 44, 37, and -15°C in the palmitate-, erucate- and oleate-enriched membranes respectively. These temperatures vary over a range of  $\pm 2$  deg. C in different preparations. In each case the transition is broad and extends 20 to 25 deg. C below the high temperature end of the transition.

The 4.15 Å diffraction is very sharp below the phase transition. After corrections are made for the intrinsic properties of the camera and the effect of specimen thickness, the angular half-width of the peak is approximately 0.2°, indicating that the diffracting regions are approximately 400 Å in extent (Guinier, 1963). Above the transition, the angular half-width of the 4.6 Å diffraction is much larger, indicating a loss of long range order.

Isolated membranes were examined in negatively stained electron microscope preparations made at temperatures above and below the thermal phase transition. No difference in morphology was evident, the membranes appearing as flattened, empty vesicles with a pebbled, irregular surface texture in both cases.

#### (b) *Low-angle scattering from membrane dispersions*

There are changes in the low-angle diffraction patterns which accompany the transition seen in the wide-angle patterns. Corrected amplitude curves ( $I + \sin \theta$  versus  $1/d$ , where  $1/d = (2 \sin \theta)/\lambda$ ) were obtained for palmitate- and erucate-enriched membranes above and below the transition.

Below the transition, three bands are seen: a strong band centred near 1/50 Å and two weaker subsidiary bands near 2/50 Å and 3/50 Å (Fig. 2). The second and third bands are of comparable intensity. The equivalent Bragg spacings of the bands are shown in Table 1. The erucate-enriched membranes give spacings which are larger than those for the palmitate-enriched membranes. Although the investigation of the low-angle spacings of the oleate-supplemented membrane diffraction bands is still in progress, the preliminary results give the spacings shown.

Above the phase transition there are two basic changes in the low-angle patterns (Fig. 3): each of the three bands moves to a smaller spacing and the third band

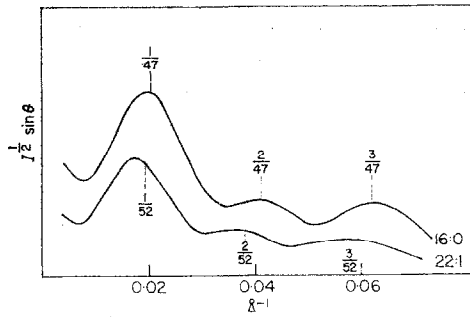


FIG. 2. Low-angle diffraction from membrane dispersions at temperatures below the thermal phase transition. The vertical axis is in arbitrary units, and the 2 curves have been scaled to separate them for comparison.

The upper curve is from palmitate (16:0)-enriched membranes at 10°C; the lower curve from erucate (22:1)-enriched membranes at 10°C.

TABLE I

*Equivalent Bragg spacings of low-angle diffraction bands from isolated membranes*

| Membrane enriched with | Band number h | Below transition  |          | Above transition  |          |
|------------------------|---------------|-------------------|----------|-------------------|----------|
|                        |               | Band spacing in Å | $D = hd$ | Band spacing in Å | $D = hd$ |
| Palmitic acid          | 1             | 50.5              | 50.5     | 44.4              | 44.4     |
|                        | 2             | 23.6              | 47.2     | 19.4              | 38.8     |
|                        | 3             | 15.7              | 47.1     |                   |          |
| Erucic acid            | 1             | 57.1              | 57.1     | 46.0              | 46.0     |
|                        | 2             | 26.2              | 52.4     | 20.5              | 41.0     |
|                        | 3             | 17.4              | 52.2     | 13.9              | 41.8     |
| Oleic acid             | 1             |                   |          |                   |          |
|                        | 2             | 23.4              | 46.8     | 20.1              | 40.2     |
|                        | 3             | 15.0              | 45.0     |                   |          |

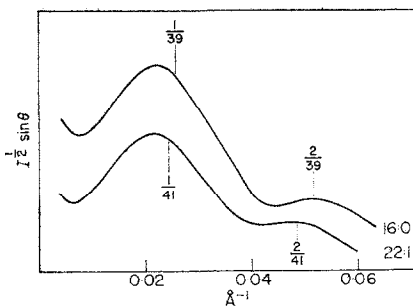


FIG. 3. Low-angle diffraction from membrane dispersions at temperatures above the thermal phase transition.

The vertical axis is in arbitrary units and the 2 curves have been scaled to separate them for comparison. The upper curve is from palmitate (16:0)-enriched membranes at 43°C; the lower curve is from erucate (22:1)-enriched membranes at 37°C.

becomes much weaker than the second. The third band is so weak that it is not recorded in the densitometer traces and can only be seen in very heavily exposed films. Again the spacings for the erucate membranes are greater than those for the palmitate membranes (see Table 1), and a preliminary measurement of the  $h = 2$  position for the oleate membranes is given.

(c) *Diffraction from partially oriented membrane arrays*

Centrifugation of membranes at temperatures below the phase transition causes them to orient roughly parallel to one another in regions of the pellet. These regions remain even after the pellet has been transferred to a glass capillary, and diffraction patterns can be obtained from them. The membranes then appear to be oriented approximately parallel to one another but not regularly spaced, and hence the diffraction pattern does not show sharp Bragg reflections but has a continuous distribution like that of the dispersions. Although the observations of oriented membranes are still in progress there are some important features of the patterns which are clear. First, the three bands have a comparable degree of angular orientation about the meridian (perpendicular to the planes of the membranes) and the 4.15 Å diffraction has angular orientation about the equator. This shows that the three bands can be related to the same orientable structural feature and that the fatty acid chains are roughly perpendicular to that feature.

Second, the presence of other contributions to the low-angle diffraction can be detected by measuring intensity profiles along the meridian and equator. Figure 4 shows data from such profiles for palmitate-enriched membranes below their phase transition.

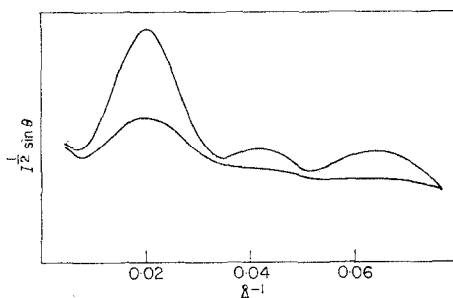


FIG. 4. Low-angle diffraction from a partially oriented array of palmitate-enriched membranes below the thermal phase transition.

The upper curve is the diffraction on the meridian, perpendicular to the planes of the membranes. The lower curve is the diffraction on the equator.

## 5. Discussion

### (a) *Hydrocarbon chain packing*

The sharp 4.15 Å diffraction from membranes below the thermal phase transition is interpreted as arising from parallel hydrocarbon chains packed in an hexagonal array with an axis-to-axis spacing of 4.80 Å. If the strong water diffraction is reduced by drying the specimen, another ring is observed at 2.4 Å, which is the next spacing on the hexagonal lattice (drying causes some changes in the low-angle diffraction, but the 4.15 Å peak remains unchanged). The packing is like that of the hexagonal phase of long-chain normal paraffins (Müller, 1932; Vand, 1953) in which the chains are fully

extended and can undergo rotational movements about their long axes. This state has not previously been known to occur in natural membranes, but it has been observed in lamellar phases of phospholipid-water mixtures (Luzzati, 1968). It is, perhaps, surprising that the presence of *cis* double-bonds does not prevent such packing; the fact that the 4.15 Å spacing is the same for oleate-, erucate- and palmitate-enriched membranes indicates that the *cis* double-bond can be accommodated without great distortion of the hexagonal lattice.

The large size of the diffracting regions, approximately 400 Å, may be compared with the membrane thickness of 75 to 90 Å obtained by electron microscopy (Terry, Engelman & Morowitz, 1967). This comparison indicates that the regions must be in the plane of the membrane, that is, with the chains approximately perpendicular to the membrane sheet. Such orientation is observed for membranes in partly ordered arrays.

There are, therefore, three lines of argument that indicate that the membrane lipids are in a bilayer (or possibly a monolayer) below the phase transition. First, the hexagonal packing giving rise to the 4.15 Å diffraction is not observed in non-lamellar phases of phospholipid-water mixtures (Luzzati, 1968). Second, the chains are oriented across the membrane as shown by the orientation of the 4.15 Å diffraction from partly oriented arrays. Third, the large size of the diffracting regions shows that the chain axes are parallel to one another over large distances. The possibility that the lipids are in a monolayer cannot be excluded on the basis of the wide-angle diffraction alone, but is eliminated by the analysis of the low-angle diffraction presented below.

Above the transition the chains are in a more fluid state. The broad peak at 4.6 Å is like that of the liquid hydrocarbons, and its increased half-width indicates a loss of long-range order compared with the state below the transition.

#### (b) *Membrane profile diffraction from dispersions*

The characteristics of low-angle diffraction from lipid bilayers have been predicted theoretically and corroborated experimentally (Wilkins *et al.*, 1971; Levine & Wilkins, 1971). These features are recognizable in the patterns from intact *Mycoplasma* membranes, and, since there are separate lines of argument that the lipids are in a bilayer below the phase transition, the mycoplasma data provide support for the theory.

Below the phase transition, a strong main band and two subsidiary bands are seen. The subsidiary bands are located at submultiples of the basic spacing  $D$ , of the main band.  $D$  is a measure of the separation of the two peaks in the electron density profile of a lipid bilayer (the head group regions). The lipid fatty acid chains are approximately perpendicular to the plane of the membrane, so that a change in the average chain length ought to be observed as a change in the peak-to-peak separation, since the dimensions of the bilayer will change. In the erucate-enriched membranes, the average chain length is approximately 20 carbons; in the palmitate-enriched case it is 16 carbons. Measurements of Corey-Pauling-Koltun models of the lipids show that a thickness difference of about 7 Å should exist. In fact,  $D = 52$  Å in the erucate case and  $D = 47$  Å in the palmitate case. The shift is in the correct direction, but somewhat smaller than expected. Nonetheless, it is significantly greater than the maximum shift expected for a monolayer. The difference may well be due to a difference in average orientation of the chains relative to the plane of the membrane induced by the presence of *cis* double-bonds in the erucate case. Preliminary confirmation of this is

provided by the fact that oleate-enriched membranes have  $D = 46 \text{ \AA}$  although the chains have an average length of 17 carbons. Furthermore, the absolute dimension of  $47 \text{ \AA}$  for the palmitate case is very close to the value of  $48 \text{ \AA}$  obtained from measurements of Corey–Pauling–Koltun models of the known *Mycoplasma* lipids (Shaw, Smith & Koostra 1968) which is based on the assumption that the chains are perpendicular to the sheet.

Above the phase transition, the bands move to smaller spacings and the third band becomes much weaker than the second. The basic form of the diffraction, however, remains the same—a strong main band with subsidiary bands at submultiples of the main band spacings. As the chains become more fluid, the dimensions of the bilayer may decrease, since their average orientation will now be further from the perpendicular to the sheet. Also the terminal methyl groups of the chains will be less well localized and the theory predicts that the third band will therefore become smaller relative to the second (compare Fig. 1(a) and (b)). These are the effects observed. Furthermore, the shift in  $D$ , with composition, is still apparent:  $D = 39 \text{ \AA}$  and  $41 \text{ \AA}$  for the palmitate- and erucate-enriched membranes, respectively.

### (c) Diffraction from oriented arrays

The lipid structure of the membrane, then, is predominantly a bilayer, but what is the arrangement of the other molecular species of the membrane, particularly the protein? The membrane is more than half protein by weight and as the protein has an electron density considerably greater than water it should contribute to the low-angle diffraction. Model calculations (Fig. 1) show that protein distributed in thick, hydrated layers on the outside of the bilayer will not affect the pattern substantially, but even these effects (primarily on the shape of the main band) are not observed. A feature of the observed diffraction which is not predicted by the bilayer theory is that the minima between the bands are non-zero (Figs 2 and 3). This could be an effect due to asymmetry of the membrane, to variation of the bilayer thickness  $D$ , or to contributions from electron density variations in the plane of the membrane, perhaps from protein structural features.

The observation of oriented membrane arrays permits a comparison of the diffraction from the membrane profile with other components of the diffraction which in general will not have the same orientation. Corrected amplitude curves from densitometer traces taken on the meridian and equator of such a pattern from palmitate-enriched membranes below the thermal phase transition are shown in Figure 4. Since the curves do not have the same profile, more than one component must be contributing to the low-angle pattern. Although some of the main band appears to be present in the equatorial diffraction, there is another component which appears to give a constant intensity in the  $I^{\frac{1}{2}} \sin \theta$  plot. Assuming that the non-bilayer diffraction is symmetrical about the origin, the meridional and equatorial traces can be compared to separate the oriented component.

Subtracting the equatorial from the meridional intensities and plotting  $(I_{\text{meridian}} - I_{\text{equator}})^{\frac{1}{2}} \sin \theta$  versus  $1/d$ , the solid curve shown in Figure 5 is obtained. Although the minima are still not zero, they are much lower. Furthermore, the third band now has a maximum greater than that of the second. If the minima are interpreted as zeros, the dashed baseline shown in Figure 5 is obtained. The difference between the dashed baseline and the experimental baseline then represents another contribution to the oriented diffraction, perhaps from asymmetrically distributed material external to

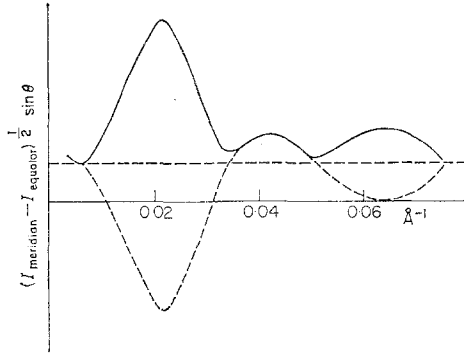


FIG. 5. Difference curve obtained from the data in Fig. 4.

The difference of intensities between the meridional and equatorial traces is used as the intensity. The dashed curve and baseline show an interpretation of the curve as the Fourier transform of a bilayer (compare Fig. 1(b)).

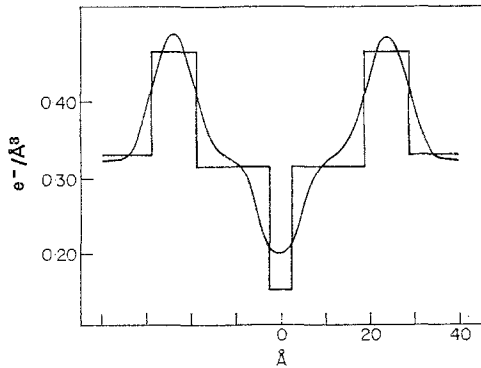


FIG. 6. A step-function model for the lipids of a palmitate-enriched membrane below the thermal phase transition is shown.

The curve superimposed on it is the Fourier inversion of the interpreted transform of Fig. 5; the vertical scale of the curve has been arbitrarily assigned to permit comparison of the general shape and the positions of prominent features of the curve with those of the step-function model. The vertical position of the model has been assigned by assuming that the electron density level far from the bilayer structure in the experimental curve is that of water.

the bilayer. Another possibility is that there are variations in thickness giving variations in  $D$ ; the averaging of zeros at several positions would give an elevated baseline. Taking the dashed baseline, the experimental curve can be interpreted to give the transform curve shown in dashed lines. This curve strongly resembles the transform of a bilayer with localized fatty acid methyl groups (see Fig. 1(b)), and Fourier inversion gives the electron density curve shown in Figure 6. It is shown superimposed on a step function model derived for a palmitate-enriched membrane bilayer without protein. The agreement is good between the model and the experimental profile.

It seems clear that the diffraction oriented on the meridian largely can be accounted for in terms of a lipid bilayer alone. If the membrane protein were present as uniform layers on the sides of the bilayer, they would be about 35 Å thick as in Figure 1(c). Most of the membrane protein is therefore not located in uniform layers on either side of the bilayer unless uniform layers are formed when the membrane is above the thermal phase transition; the shape of the first diffraction band above the transition

does not indicate the formation of such layers. Some of the lipid head groups would then be exposed to the aqueous environment as has been suggested on the basis of phospho-lipase digestion experiments (Lenard & Singer, 1968). Further definition of the distribution of membrane protein must await interpretation of the low-angle diffraction which does not arise from the lipid bilayer. The present data do not exclude the possibility that the membrane contains non-lipid structures penetrating the bilayer, such as the particles observed in fracture faces of frozen membranes (Branton, 1966), except that such particles cannot be present in the ordered hydrocarbon regions below the thermal phase transition.

(d) *Some restrictions on possible lipid-protein interactions*

There is good evidence that the palmitate-enriched lipid fatty acid chains are perpendicular to the plane of the bilayer regions below the thermal phase transition. The area per lipid molecule must then be approximately twice the cross-sectional area of a single hydrocarbon chain in the hexagonal phase, or  $40 \text{ \AA}^2$ . In the case of the erucate-enriched membranes, the fatty acid chains are slightly tilted from the perpendicular below the transition. Comparing the thickness of the hydrocarbon region obtained from model building ( $45 \text{ \AA}$ ) with that measured by taking  $10 \text{ \AA}$  for the head group contribution to  $D$  ( $D - 10 = 42 \text{ \AA}$ ) shows that there is an average tilt of about  $20^\circ$  from the perpendicular. This tilt only increases the area per lipid molecule to  $43 \text{ \AA}^2$ . Such a close packing of the lipid heads in the bilayer regions excludes the possibility that protein can make contact with the hydrocarbon region by penetrating past the heads, and the protein is then restricted to interaction with the lipid heads alone in these regions.

Above the thermal phase transition such a precise measure of the area per lipid molecule cannot be made; however, if the individual  $\text{CH}$ ,  $\text{CH}_2$ , and  $\text{CH}_3$  groups of the fatty acids are taken as having approximately the volumes that they occupy in liquid hydrocarbons ( $\text{CH} = 21.5 \text{ \AA}^3$ ,  $\text{CH}_2 = 27.0 \text{ \AA}^3$ ,  $\text{CH}_3 = 54 \text{ \AA}^3$ ; Engelman, 1969), areas per lipid molecule can be calculated. The carbonyl carbon is in a region of high electron density and is not considered as part of the hydrocarbon layer, so for the average chain of the palmitate (16:0)-enriched membrane the equivalent liquid hydrocarbon volume is  $V = 54 + 14(27) = 432 \text{ \AA}^3$ . Allowing  $10 \text{ \AA}$  for the lipid heads, the hydrocarbon region is  $D - 10 = 39 - 10 = 29 \text{ \AA}$  across, so the area per chain is  $432/14.5 = 30 \text{ \AA}^2$  since there are two chain lengths across the bilayer. The area per lipid is therefore about  $60 \text{ \AA}^2$  for the palmitate-enriched membranes above the transition. A similar calculation gives an area per lipid of about  $70 \text{ \AA}^2$  for the erucate-enriched membrane above its transition. These areas per lipid molecule differ significantly from each other and from the area per molecule of 40 to  $43 \text{ \AA}^2$  below the thermal phase transition. It follows that whatever the nature of the lipid-protein interaction in the bilayer regions of the membrane is, it cannot require a highly specific area per lipid molecule. Moreover, the areas above the transition are similar to those found for comparable lipids in monolayers at an air-water interface, and to those found for lamellar phases of phospholipid-water mixtures (60 to  $72 \text{ \AA}^2$ ; Luzzati, 1968) in which the lipid chains give a broad  $4.6 \text{ \AA}$  diffraction band. Interaction of protein with the lipid in the bilayer regions does not appear to alter the packing of the lipid molecules.

(e) *Conclusions*

In summary, the sharp wide-angle diffraction at  $4.15 \text{ \AA}$  indicates that a lipid bilayer or monolayer is present below the phase transition. Features predicted for lipid

bilayer diffraction are recognized in the low-angle patterns both above and below the phase transition, and the differences are as expected. The interpretation of the low-angle patterns is confirmed by changing the average fatty acid chain length and observing changes in the diffraction produced by changes in the width of the bilayer. The changes are as predicted from the bilayer theory and the lipid compositional shift. It is concluded that the predominant lipid structure in the membrane is a bilayer.

The main features of the oriented diffraction from partly ordered arrays of membranes below the phase transition can be accounted for by the bilayer alone, so the majority of the membrane protein is not present in uniform layers on either side of the lipid bilayer regions. The small area per lipid molecule below the transition shows that protein cannot penetrate the lipid heads to make hydrophobic contact with the hydrocarbon region. Above the phase transition the area per lipid molecule is comparable to that expected for an isolated lipid bilayer; protein interactions do not constrain the lipid packing greatly. These restrictions on the nature of the protein distribution and the nature of the lipid bilayer-protein interaction impose important constraints on models for membrane structure.

I thank Dr C. W. F. McClare, Dr A. E. Blaurock, Professor M. H. F. Wilkins, and Professor Sir John Randall for their generous help and useful discussions. I was supported by a postdoctoral fellowship from the U.S. National Institute of Arthritis and Metabolic Diseases.

#### REFERENCES

- Benson, A. A. (1966). *J. Amer. Oil Chemists' Soc.* **43**, 265.  
 Branton, D. (1966). *Proc. Nat. Acad. Sci., Wash.* **55**, 1048.  
 Danielli, J. F. & Davson, H. (1935). *J. Cell Physiol.* **5**, 495.  
 Elliott, A. (1965). *J. Sci. Inst.* **42**, 312.  
 Elliott, G. F. & Worthington, C. R. (1963). *J. Ultrastructure Res.* **9**, 166.  
 Engelman, D. M. (1969). *Nature*, **223**, 1279.  
 Engelman, D. M. (1970). *J. Mol. Biol.* **47**, 115.  
 Gorter, E. & Grendel, F. (1925). *J. Exp. Med.* **41**, 439.  
 Guinier, A. (1963). *X-ray Diffraction*. San Francisco and London: Freeman.  
 Kavenau, J. L. (1966). *Fed. Proc.* **25**, 1096.  
 Koltun, W. C. (1965). *Biopolymers*, **3**, 665.  
 Korn, E. D. (1966). *Science*, **153**, 1491.  
 Lenard, J. & Singer, S. J. (1966). *Proc. Nat. Acad. Sci., Wash.* **56**, 1828.  
 Lenard, J. & Singer, S. J. (1968). *Science*, **159**, 738.  
 Levine, Y. K. & Wilkins, M. H. F. (1971). *Nature*. In the press.  
 Lucy, J. A. (1964). *J. Theoret. Biol.* **7**, 360.  
 Luzzati, V. (1968). In *Biological Membranes*, ed. by D. Chapman, p. 71. New York: Academic Press.  
 Marinetti, G. V. (1962). *Biochemistry*, **1**, 350.  
 McElhaney, R. N. & Tourtellotte, M. E. (1969). *Science*, **164**, 433.  
 Müller, A. (1932). *Proc. Roy. Soc. A*, **133**, 514.  
 Razin, S. (1964). *J. Gen. Microbiol.* **36**, 451.  
 Razin, S., Morowitz, H. J. & Terry, T. M. (1965). *Proc. Nat. Acad. Sci., Wash.* **54**, 219.  
 Razin, S., Tourtellotte, M. E., McElhaney, R. N. & Pollack, J. D. (1966). *J. Bact.* **91**, 609.  
 Reinert, J. C. & Steim, J. (1970). *Science*, **168**, 1580.  
 Reiss-Husson, F. & Luzzati, V. (1964). *J. Phys. Chem.* **68**, 3504.  
 Robertson, J. D. (1959). In *Biochemical Symposium no. 16*, p. 3. London: Biochemical Society.  
 Shaw, N., Smith, P. F. & Koostera, W. L. (1968). *Biochem. J.* **107**, 329.

- Smiles, S. (1910). In *The Relation between Chemical Composition and some Physical Properties*. London: Longman and Green.
- Stein, J. M., Reinert, J. C., Tourtellotte, M. E., McElhaney, R. N. & Rader, R. L. (1969). *Proc. Nat. Acad. Sci., Wash.* **63**, 109.
- Stoeckenius, W. & Engelman, D. M. (1969). *J. Cell Biol.* **42**, 613.
- Terry, T. M., Engelman, D. M. & Morowitz, H. J. (1967). *Biochim. biophys. Acta*, **135**, 391.
- Vand, V. (1953). *Acta Cryst.* **6**, 797.
- Wilkins, M. H. F., Blaurock, A. E. & Engelman, D. M. (1971). *Nature*, In the press.